Genetic and environmental factors determining heterogeneity in preservation stress resistance of Aspergillus niger conidia

Seekles, S.J.

CHAPTER 8

The impact of cultivation temperature on the transcriptome, proteome and heat resistance of *Aspergillus niger* conidia

Sjoerd J. Seekles, Maarten Punt, Tom van den Brule, Mark Arentshorst, Gertjan Kramer, Winfried Roseboom, Gwen Meuken, Véronique Ongenae, Jordy Zwerus, Stanley Brul, Jan Dijksterhuis, Han A. B. Wosten, Robin A. Ohm, Arthur F.J. Ram

Manuscript in preparation

Abstract

Asexual spores (conidia) of filamentous fungi are reported to have increased heat resistance when cultivated at higher temperatures, which is shown to be associated with trehalose accumulation. In this study, we show that the heat resistance of conidia from food spoiler *Aspergillus niger* also increases when cultivated at increased temperatures. Phenotypic analysis of *A. niger* mutants devoid from any trehalose due to the deletion of all three trehalose 6-phosphate synthase genes (Δ*tpsABC*) showed that the observed increase in heat resistance was not solely due to trehalose accumulation inside conidia. We investigated the possibility that protective proteins could cause the observed increase in conidial heat resistance. Several strains lacking putative protective proteins were created, and subsequently investigated for their role in conidial heat resistance. The conidia an *A. niger* strain lacking NRRL3_02725, a Hsp104 homologue, was found to be in general more heat sensitive compared to the parental strain, but none of the knock-out strains in genes encoding putative protective proteins, including Δ*NRRL3_02725*, could explain the heat resistance increase seen in conidia due to cultivation at increased temperatures. Therefore, transcriptome and proteome studies were conducted on dormant conidia cultivated at 28°C, 32°C and 37°C in order to find possible candidate protective proteins. We show that only two genes encoding putative *hsp26/42*-type heat shock proteins, NRRL3_04002 and NRRL3_10215, are upregulated in both the transcriptome and proteome datasets. These two genes are promising candidates for the observed heat resistance increase in conidia when cultivated at increased temperature.

Introduction

Filamentous fungi are among the most common food spoilage microbes found across food sectors, and are known spoilers of highly processed food products [1,2]. Food spoiling filamentous fungi can be classified in five different groups [3]: Xerophilic fungi that can grow on water activities below 0.85 [4], anaerobic fungi that can grow without oxygen [5], psychrophilic/psychrotolerant fungi that can grow or survive at or below 0 °C [6], preservative resistant fungi that can grow in the presence of preservatives [7] and heat resistant fungi capable of surviving high temperature treatments up to 90°C for 25 minutes [8]. The group of heat resistant molds (HRM) produce heat resistant sexual spores (ascospores) known to survive pasteurization treatments of 65°C to 70°C [8–10]. These ascospores are generally regarded as the most heat resistant fungal structure and have therefore been studied more than asexual fungal spores (conidia) with regards to food spoilage [11]. However, conidia, in contrast to ascospores, are survival structures that are airborne and produced in huge amounts. Virtually every cubic meter of air contains these asexual fungal spores [12–15]. Therefore, food spoilage by conidia is more prevalent and thus seen in many food sectors, such as in the production of animal feed, dairy products and fruit juices [16–19]. Recently, the most heat resistant conidia to date were described as produced by *Paecilomyces variotii* DTO 217-A2 which survive up to 22 minutes at 60 °C which is within the margins of common milk thermization protocols [20,21].

Previous research has shown the impact of conidial age, cultivation medium as well as cultivation temperature on the stress resistance of resulting conidia [22–26] (and Chapter 7). Conidial populations of *Aspergillus fumigatus* and *Penicillium roqueforti* harvested from plates incubated at a high temperature were more heat resistant than conidial populations harvested from plates incubated at a low temperature [23,25].

The heat resistance of conidia is at least partially due to its high intracellular concentrations of compatible solutes [21,25,27–29]. Recently, we have shown that *A. niger* conidia lacking both trehalose and most mannitol are comparable to young conidia, and

survive up to ~5 minutes at 54°C (Chapter 7). Additionally, other protective molecules, such as heat shock proteins (HSPs) and dehydrins, accumulate inside conidia of *A. niger* and *A. fumigatus* as found in transcriptomic and proteomic data, which are speculated to impact conidial stress resistance [30–33]. Indeed, expression of heat shock proteins is induced in conidia when heat treated for 4 hours during conidiation, suggesting that these protective proteins play a role in the increased heat resistance of conidia as an adaptive response to the shift towards a high temperature environment [34].

In this research, we show the impact of cultivation temperature during conidiation on the heat resistance of the resulting conidia of *A. niger*. We show that cultivation at higher temperatures increases the heat resistance of conidia. This correlates with an increase in trehalose content, which has also has been observed in other filamentous fungi [23,25]. However, conidia of a deletion strain incapable of producing trehalose still increased in heat resistance when cultivated at higher temperatures, suggesting involvement of other molecules. Deletion mutants lacking candidate protective proteins were made, however all knock-out mutants analysed showed conidia with increased heat resistance when cultivated at higher temperatures. Therefore, we compared the transcriptome and proteome data of dormant conidia cultivated at 28°C, 32°C and 37°C to find potential proteins involved in conidial heat resistance. The possible role of two potential candidate heat shock proteins, NRRL3_04002 and NRRL3_10215, which are most likely involved in the heat resistance increase of conidia when cultivated at higher temperatures is discussed.

Results

Conidia cultivated at higher temperatures show increased heat resistance

The impact of cultivation temperature, meaning the temperature at which conidiation takes place, on the heat resistance of conidia of *A. niger* was investigated. Previous reports have shown that an increase in heat resistance of conidia cultivated at higher temperatures correlates with increased trehalose concentrations [23,25]. In order to investigate this correlation, conidia from strains N402 (parental) and SJS126 (*ΔtpsABC*) unable to produce trehalose (Chapter 7) were harvested from plates that had been incubated at either 28°C or 37°C for 8 days and subsequently analysed for internal compatible solute composition and heat resistance (Figure 8.1). Additionally, heat resistance changes due to cultivation temperature (28°C, 32°C and 37°C) of conidia from *A. niger* N402 were further quantified in a heat inactivation experiment to determine decimal reduction values (D-values), by following conidial heat inactivation through time (Figure 8.2). The D_{57}-values of N402 conidia cultivated at 28°C, 32°C and 37°C were 6.5 ± 1.9 minutes, 9.7 ± 0.5 minutes and 17.0 ± 0.4 minutes, respectively (Table 8.1). Statistical analysis confirmed that *A. niger* conidia cultivated at 37°C are significantly more heat stress resistant than those cultivated at 28°C and 32°C ($p<0.05$). No significant difference was detected between D_{57}-values of *A. niger* conidia cultivated at 28 °C and 32 °C ($p=0.45$). Taken together, both experiments show that conidia of *A. niger* N402 harvested from plates cultivated at 37°C, are more heat resistant than conidia harvested from plates cultivated at 28°C. This increase in heat resistance due to increased cultivation temperature was also not specific for the N402 *A. niger* strain that is often used in lab studies [35,36] and also observed in two randomly picked wild-type *A. niger* strains CBS112.32 and CBS147347 (Figure 8.S1), showing the consistency of the increase in heat resistance due to increased cultivation temperature among *A. niger* strains. An increase in intracellular trehalose levels was measured in conidia of lab strain N402 when cultivated at higher temperatures (Figure 8.1B), suggesting that the accumulation of trehalose upon cultivation at higher temperatures is conserved among *A. niger*,

A. fumigatus and *P. roqueforti* [23,25]. As shown earlier and confirmed here, trehalose levels are undetectable in the *ΔtpsABC* strain (SJS126) and its conidia have lower heat resistance than wild type N402, but interestingly still produced conidia with increased heat resistance upon cultivation at higher temperatures (Figure 8.1). Therefore, the observed increase in conidial heat resistance due to higher cultivation temperature is not solely due to an increase in the amount of intracellular trehalose. We hypothesized that the observed change in heat resistance is instead due to the accumulation of currently unknown protective proteins.

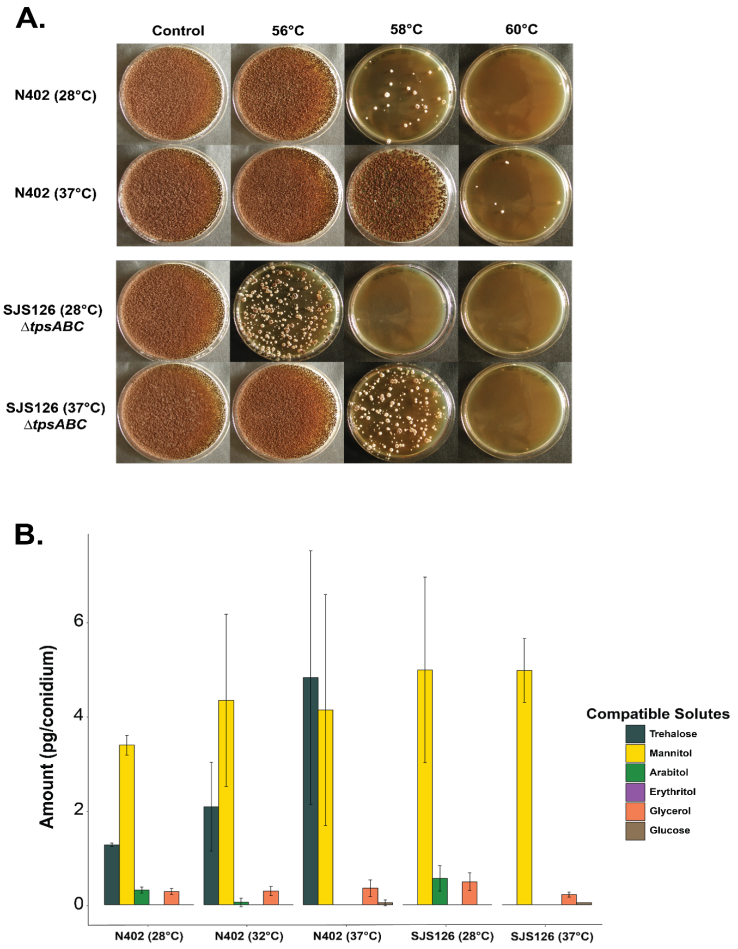

Figure 8.1. Heat resistance increase due to increased cultivation temperature of N402 and the trehalose deficient mutant SJS126. A. Conidia were harvested from mycelium cultivated at 28°C or 37°C. Heat resistance of lab strain N402 is higher than trehalose deficient mutant SJS126 (ΔtpsABC) as was shown previously (Chapter 7). Conidia harvested from mycelium cultivated at

37°C are more heat resistant than conidia harvested from mycelium cultivated at 28°C in both the lab strain N402 and the trehalose deficient mutant SJS126. B. The heat resistance increase in the lab strain N402 correlates with an increase observed in the amount of trehalose accumulated in the conidia. However, the conidia of trehalose deficient mutant SJS126 do not accumulate extra compatible solutes (the strain is incapable of biosynthesizing trehalose) when cultivated at 37°C, while these conidia still have an increased heat resistance. Therefore, the heat resistance increase observed of conidia cultivated at higher temperatures is not solely due to accumulation of trehalose.

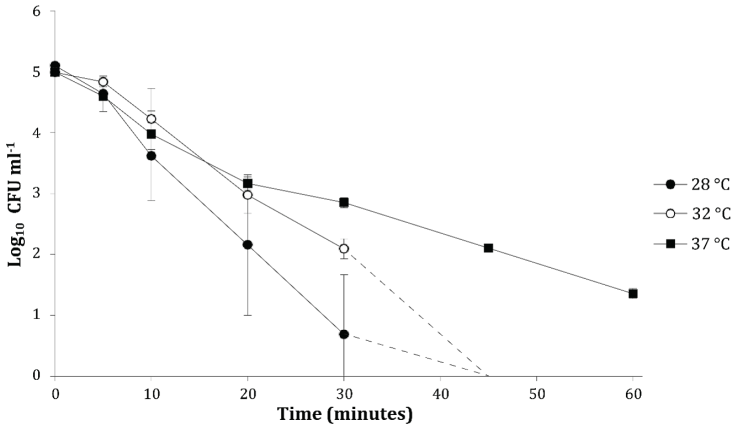

Figure 8.2. Heat inactivation curves of A. niger N402 conidia cultivated at 28°C, 32°C and 37°C. The heat inactivation experiment was performed in a 57°C water bath. Data is based on biological duplicates. After 45 minutes, none of the conidia harvested from plates cultivated at 28°C or 32°C survived the heat treatment, a 5-log reduction in microbial load was observed (less than 1 in 105 conidia survive). In contrast, conidia harvested from plates that were incubated at 37°C survived up till 60 minutes of heat treatment, a 3-log reduction in microbial load was observed (1 in 103 conidia survive). These data indicate that a population of A. niger conidia harvested from mycelium that was incubated at a high(er) temperature has a high(er) heat resistance. D-values were calculated based on linear regression lines and given in Table 8.1.

Table 8.1. D_{57}-values of *A. niger* N402 conidia cultivated at 28°C, 32°C or 37°C. These D-values were calculated based on the log-linear regression model and is based on two biological replicates.

Cultivation temperature	D_{57}-value ± SD (minutes)
28 °C	6.5 ± 1.9
32 °C	9.7 ± 0.5
37 °C	17.0 ± 0.4

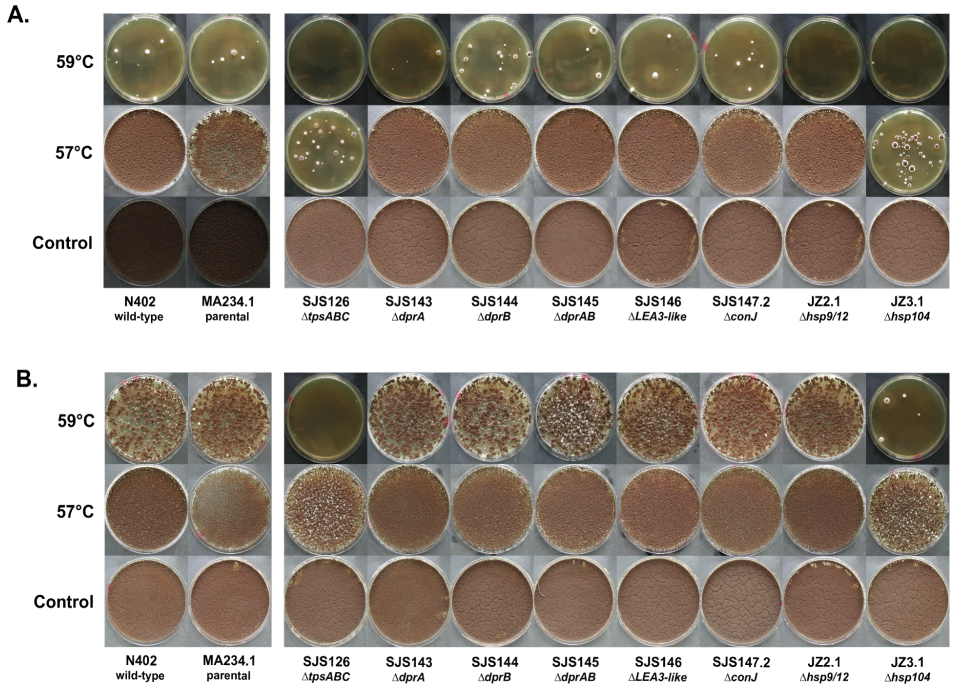

Figure 8.3. Heat resistance of knock-out mutants lacking protective proteins. Knock-out strains were grown for 8 days at 28°C or 37°C on MEA plates. Conidia were harvested and subsequently 106 conidia were heat treated and plated to count colony forming units (CFUs). Heat treatment was done for 10 minutes at either room temperature (control), 57°C or 59°C. All samples were measured in biological triplicates. A. heat treatment of conidia harvested from mycelium cultivated at 28°C. Knock-out mutants lacking protective proteins are comparable in heat resistance to their parental strain MA234.1, except for the Δhsp104 mutant JZ3.1. Conidia of strain SJS126 that lacks trehalose are sensitive to heat, as was shown before (Chapter 7). B. Heat treatment of conidia harvested from mycelium cultivated at 37°C. Heat resistance of conidia from all knock-out strains increased when compared to those cultivated at 28°C as seen by the increased amount of colony forming units after a 10 minutes 59°C heat treatment.

8

Conidia from deletion mutant *Δhsp104* are more sensitive to heat stress, but still show increased heat resistance upon cultivation at higher temperatures

Deletion mutant strains of *A. niger* were made lacking genes coding for putative protective proteins. The gene selection was based on putative protective proteins shown to accumulate high amount of mRNA inside dormant conidia of *A. niger* based on previous transcriptomic data [30], and the details on the six target genes can be found in Table 8.2. The heat resistance of conidia of strains SJS143 (*ΔNRRL3_01479*; *ΔdprA*), SJS144

(*ΔNRRL3_01479*; *ΔdprB*), SJS145 (*ΔNRRL3_01479, ΔNRRL3_01479*; *ΔdprA*B), SJS146 (*ΔNRRL3_05684*; *ΔLEA3-like*), SJS147.2 (*ΔNRRL3_02511*, *ΔconJ*), JZ2.1 (*ΔNRRL3_11620*; *Δhsp9/12*) and JZ3.1 (*ΔNRRL3_02725*; *Δhsp104*) was compared to that of the parental strain MA234.1 (*ΔkusA*), lab strain N402 and the trehalose deficient knock-out strain SJS126 (*ΔtpsABC*) (Figure 8.3). Strain JZ3.1 (*Δhsp104*) produced conidia with reduced heat resistance, with no observed change in internal compatible solutes when compared to its parental strain (Figure 8.S2). Therefore, the putative Hsp104 homologue was found to contribute to conidial heat resistance. However, all knock-out strains, including JZ3.1 (*Δhsp104*), continued to show an increased heat resistance when conidia were cultivated at 37°C (Figure 8.3B) versus 28°C (Figure 8.3A). None of these six putative protective proteins could explain the observed increase in heat resistance due to increased cultivation temperature.

Table 8.2. Six target genes coding for putative protective proteins. These six putative protective proteins were all highly expressed in dormant *A. niger* conidia in a previous study by van Leeuwen et al. [30]. The putative gene names were used throughout the manuscript instead of gene numbers to help guide the reader.

Gene name used	NRRL3-number	An-number	Description	Additional information
dprA	NRRL3_01017	An14g05070	Dehydrin-like protective proteins, homologoues DprA & DprB, found in conidia of *Aspergillus fumigatus*, are involved in multiple stress responses including osmotic, pH and oxidative stress[62].	BLASTp reveals DprA from *A. fumigatus* has 71.8% and 56.8% homology with NRRL3_01017 and NRRL3_01479, respectively. Similarly, DprB from *A. fumigatus* has 74.4% and 61.4% homology with NRRL3_01017 and NRRL3_01479, respectively.
dprB	NRRL3_01479	An13g01110	Dehydrin-like protective proteins, homologoues DprA & DprB, found in conidia of *Aspergillus fumigatus*, are involved in multiple stress responses including osmotic, pH and oxidative stress [62].	BLASTp reveals DprA from *A. fumigatus* has 71.8% and 56.8% homology with NRRL3_01017 and NRRL3_01479, respectively. Similarly, DprB from *A. fumigatus* has 74.4% and 61.4% homology with NRRL3_01017 and NRRL3_01479, respectively.

Gene name used	NRRL3-number	An-number	Description	Additional Information
LEA3-like	NRRL3_05684	An02g07350	Described as a LEA3-like protein, LEA3 proteins are known to protect plants against desiccation [30,63] which coincided with one round of mitosis.	Has a 'CsbD-like protein' domain which are thought to be stress response proteins in bacteria.
conJ	NRRL3_02511	An01g10790	Name derived from conidiation specific factor 10. Highly expressed in dormant conidia of *A. niger* and known in *A. nidulans* and *A. fumigatus* to be important for spore viability [64]. Deletion mutants lacking multiple *con* genes accumulate more of the compatible solutes erythritol and glycerol.	In *Neurospora crassa*, *A. nidulans* and *A. fumigatus* no phenotype is observed in single knock-out deletion mutants. Only when multiple *con* genes are deleted are spore viability and compatible solute levels affected.
hsp9/12	NRRL3_11620	An06g01610	Best homologue to Hsp9 and Hsp12 known from yeast species. This heat shock protein is known to stabilize the plasma membrane in yeast [46,65].	
hsp104	NRRL3_02725	An01g13350	Best homologue to Hsp104 known from yeast. This heat shock protein is important for thermotolerance in yeast [37, 48, 66].	This protein is known to have interplay with trehalose, meaning that if the protein is deleted, trehalose is accumulated inside the yeast cell as compensation. Only when both trehalose and Hsp104 are abolished is the cell sensitive to heat stress.

Transcriptome and proteome analysis reveals the upregulation of two *hsp26/42* type heat shock proteins

In order to investigate which proteins are potentially involved in the observed change in heat resistance between conidia cultivated at different temperatures, a transcriptome and proteome study was conducted comparing the contents of dormant conidia cultivated for 8 days at 28°C, 32°C and 37°C. A principal component analysis was done on both the transcriptome and proteome datasets, showing in both cases that the largest differences were caused by the 37°C condition, and that the data belonging to the 28°C and 32°C conditions were fairly similar (Figure 8.S3). Therefore, the main comparison discussed in this study are the transcriptome and proteome differences between conidia

cultivated at 28°C versus 37°C. In total, 666 genes and 26 proteins were found significantly upregulated, while 783 genes and 34 proteins were found significantly downregulated in the transcriptome dataset when comparing 37°C conidia versus 28°C conidia. Log_2 fold changes (Log_2FC) were calculated for both the transcriptome and proteome datasets and subsequently plotted against each other (Figure 8.4). Genes located in the top-right corner are upregulated in the 37°C cultivated conidia in both the transcriptome and proteome dataset. Only two genes are significantly upregulated in both the transcriptome and proteome dataset, NRRL3_04002 and NRRL3_10215, which are both putative small heat shock proteins of the *hsp26/42* type. All 60 proteins that were significantly more, or less, present in conidia cultivated at 37°C (represented by blue, pink and red dots in Figure 8.4) are listed in Table 8.S1. Additionally, an enrichment study was performed investigating the annotation terms that were over- and under-represented in the 666 genes that were upregulated and the 783 genes that were downregulated. Overall, no clear biologically relevant changes could be distilled from these over- and under-represented annotation terms.

We investigated the transcriptome and proteome changes of all putative chaperones, as well as some other putative protective proteins such as hydrophobins, catalases and superoxide dismutases as these genes/proteins are most likely responsible for the increased heat resistance of conidia described above (Table 8.S2). At the top of Table 8.S2 the genes that were deleted in this study based on previously found high expression inside conidia by van Leeuwen *et al.* [30] (Figure 8.3 & Table 8.2) are listed. Indeed, the newly obtained transcriptome dataset of dormant conidia confirms that these genes are highly expressed as seen by the high baseMean DESeq2 values of these six genes. Additionally, we show that these six genes have high LFQ intensity values, indicating that the dormant conidia also contain a high amount of these proteins. Even though they are present in relatively high amounts, none of these six proteins show a significant fold change in the proteome dataset between 28°C cultivated conidia and 37°C cultivated conidia. As described above (Figure 8.4), there were only two chaperones that showed both significantly more transcript and protein in the conidia cultivated

at a high temperature (37°C) versus conidia cultivated at a low temperature (28°C). Therefore, NRRL3_04002 and NRRL3_10215, make likely candidates for the observed differences in heat resistance between conidia cultivated at a high temperature (37°C) versus a low temperature (28°C).

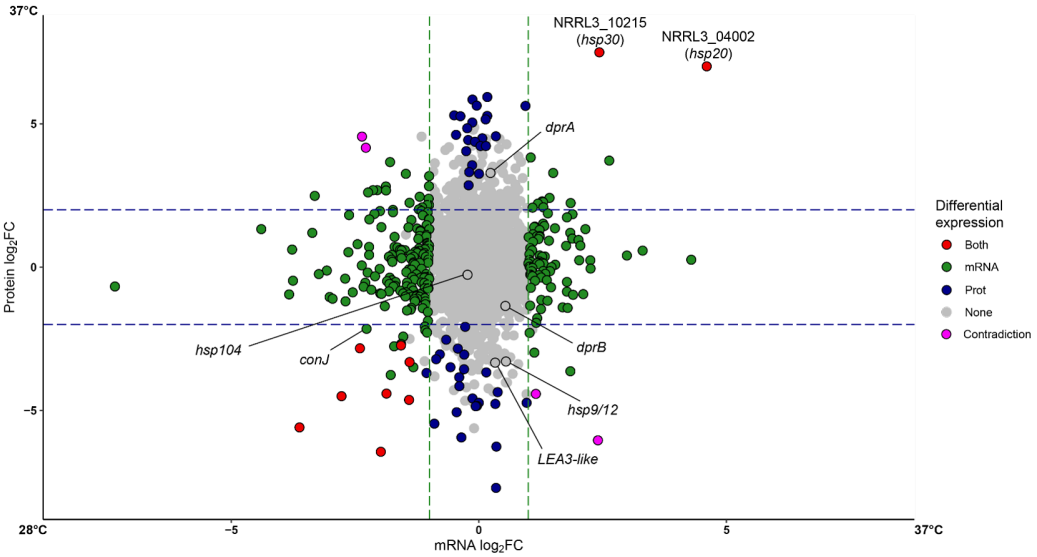

Figure 8.4. Comparison of both transcriptome and proteome fold changes of genes between conidia (37°C) and conidia (28°C). Genes having significant changes in expression (green), significant changes in protein amounts (blue) or both (red) between dormant conidia harvested from a plate cultivated at 37°C and 28°C are listed here. This graph contains only information of 2381 genes, of which proteome data was obtained, out of in total 11846 genes present on the A. niger NRRL3 genome. Only two genes and their corresponding proteins are significantly more present in the form of transcript and protein in 37°C cultivated conidia versus 28°C (NRRL3_04002 and NRRL3_10215). Therefore, these two putative heat shock proteins make excellent candidates for the observed difference in heat resistance between these two types of conidia.

Discussion

In this study we show that cultivation temperature during conidiation increases the heat resistance of the resulting conidia of *A. niger*. This phenomenon has also been observed in other filamentous fungi, including pathogenic (*A. fumigatus* [23]) and food spoilage fungi (*A. nidulans* and *P. roqueforti* [25,34]), indicating an evolutionary conserved trait of these fungi. The increase in heat resistance of conidia due to cultivation at increased temperatures has been shown to additionally correlate with an increase of internal trehalose in *A. fumigatus* and *P. roqueforti* [23,25] and was also found this study, indicating a conserved response of conidia of filamentous fungi. However, a trehalose deficient knock-out strain SJS126 (constructed previously Chapter 7) still produced conidia with increased heat resistance despite having no increased amount of internal trehalose. This indicates that molecules or proteins other than trehalose play a role in this observed increase in conidial heat resistance.

Previous reports indicated that various protective proteins accumulate inside conidia, which can potentially influence conidial stress resistance [30,31]. Therefore, deletion mutants of six putative protective proteins were constructed to investigate whether these protective proteins impact conidial heat resistance and could explain the increase in heat resistance of conidia when cultivated at higher temperatures. The deletion of a gene coding for a Hsp104 homologue resulted in conidia with lowered heat resistance (Figure 8.2). Heat shock protein 104 has been best described in *S. cerevisiae* and is a known factor in heat tolerance in this species [37]. In *S. cerevisiae*, both trehalose and protein chaperones, such as Hsp12 and Hsp104, are important for protecting against protein aggregation and are involved in proper protein refolding after damage [38,39]. It is interesting to note that Hsp104 is known to be regulated by master regulator Heat Shock Factor 1 (HSF1), a transcription factor which is key in *S. cerevisiae* for the stress response against heat [40]. The mRNA and the encoded protein of the best homologue of this transcription factor in *A. niger* (NRRL3_07278) are also present in dormant conidia of *A. niger* according to our transcriptome and proteome data (Table 8.S2). Attempts

to create a knock-out strain lacking NRRL3_07278were unsuccessful and transformants grew only as heterokaryons and were very sickly (data not shown), which suggests that deletion of this gene is lethal. Indeed, transcription factor HSF1 is known to regulate many heat shock proteins, such as Hsp70 and Hsp90, some of which are required for cell viability, and deletion mutants of HSF1 were also not viable in *S. cerevisiae*, *Candida albicans* and *A. fumigatus* [41–44]. To circumvent the lethality in *A. fumigatus*, a mutant strain was constructed in which the HsfA transcription factor was expressed from a inducible promoter. Under low-inducing conditions several genes encoding heat shock proteins were found to be downregulated including Hsp104. Interestingly, *hsp30/42* (Afu3g14540) and *hsp20/26* (Afu5g10270), best homologues of NRRL3_04002 (putative *hsp20*) and NRRL3_10215 (putative *hsp30*), were also regulated by HsfA in *A. fumigatus*.

Both trehalose and protein chaperones, like heat shock proteins, have been shown to contribute to the heat resistance of *S. cerevisiae* cells. Interestingly, researchers have suggested that trehalose might be a better chaperone than many of the protein chaperones, giving better protection against protein aggregation when studying long-term survival [45]. The yeast cell responds when faced with a lack of the protein chaperones by accumulating additional trehalose and vice versa, suggesting that the loss of one of these heat resistance elements is compensated by increasing another [46–48]. However, in our study the *Δhsp104 A. niger* strain showed altered heat resistance of conidia (Figure 8.2), but no change in internal trehalose concentration (Figure 8.S3) indicating no compensatory mechanism. Other strains lacking putative protective proteins such as Hsp9/12 also did not show an increased accumulation of trehalose inside conidia. This indicates that some protective proteins do protect against heat stressors in conidia, such as Hsp104, but do not show this interplay with trehalose, at least when analyzed inside dormant conidia. Unfortunately, although conidia of the *Δhsp104* strain show increased sensitivity towards heat stress, all conidia of deletion strains analysed in this study still showed increased heat resistance when cultivated at higher temperatures. Therefore, Hsp104 is not responsible for the increased resistance of conidia in response

to cultivation at higher growth temperatures.

To identify possible candidate proteins involved in the acquired heat resistance by cultivation at higher temperatures, we performed both transcriptome and proteome studies on dormant conidia of *A. niger* cultivated at 28°C, 32°C or 37°C. When comparing conidia cultivated at 37°C with conidia cultivated at 28°C only two genes were more prevalent in both transcriptome and proteome data, NRRL3_04002 and NRRL3_10215, which both putatively code for heat shock proteins. Gene NRRL3_04002 is the best homologue of the *hsp20* gene (AN10507) and NRRL3_10215 is the best homologue of three *hsp30/hsp26* genes (AN2530, AN3555 and AN7892) of *A. nidulans* FGSC A4. Recently, conidia of *A. nidulans* have been described as responsive to their environment while still attached to the spore chain, thereby potentially creating individual differences between conidia dependent on environmental cues during the conidiation process [34]. Wang et al. describe how multiple heat shock proteins, but mainly two genes, *hsp26* (AN7892) and *hsp30* (AN2530), are significantly upregulated when conidia attached to the spore chain are heat treated for 4 hours in *A. nidulans*. This again emphasizes the potential role of these two small heat shock proteins in the heat resistance of conidia as a response to the high temperatures of the environment. Additionally, this finding suggests that these two heat shock proteins could potentially be accumulated after conidial formation, as is also seen with compatible solute accumulation in *A. niger* (Chapter 7).

Materials and Methods

Strains, cultivation conditions and media used

The *A. niger* strains were cultivated on malt extract agar plates (MEA, Oxoid) for 8 days unless noted otherwise. The cultivation temperature experiments were done on lab strain *A. niger* N402. Plates were inoculated homogenously using sterilized glass beads. For every experiment, conidia were freshly harvested using sterilized physiological salt buffer (PS; 0.9% NaCl, 0.02% Tween 80 in demi water). A sterilized cottonbud was used to scrape the conidia off the plate, and the spore suspension was subsequently filtered using a sterilized filter (Amplitude Ecocloth, Contec) to filter out mycelial fragments.

Heat treatment assays

Heat treatment assays were performed to investigate the heat resistance of dormant conidia. Conidia were freshly harvested, counted in a cell counter (BioRad) and subsequently diluted until 10^6 conidia / 100 µL. PCR tubes were filled with 100 µL conidial suspension and heat treated for 10 minutes in a thermocycler, the lid temperature was fixed at 60°C. After heat treatment, the 100 µL conidial suspensions were plated on MEA plates with 0.05% Triton X-100 (Sigma). Pictures were taken after 5 days of growth at 28°C.

Heat inactivation experiments using a water bath (Julabo) were done inside Erlenmeyer flasks at 54°C. In short, each Erlenmeyer contained 19.8 mL PS buffer with a sterilized stirring bean which was spinning at 180 rpm inside the heated water bath. Temperatures were checked inside an extra testing Erlenmeyer by using thermometers, and care was taken to ensure the PS buffer temperature was at 54 °C +- 0.1 °C. At t = 0 the Erenmeyers were inoculated with 200 uL of conidial suspension (10^8 conidia / mL). At pre-determined time points 1.5 mL samples were taken, transferred to 2 mL Eppendorf tubes and instantly put on ice. These samples were diluted to be able to plate 10^2, 10^3, 10^4 and 10^5 conidia per plate. Plates were incubated for 7 days after which colony forming units (CFUs) were counted for each time point. D-values were calculated using

a log-linear fit.

Sample preparation and HPLC analysis

HPLC analysis was done following a previously established protocol [21]. In short, 10^8 conidia inside a 2 mL Eppendorf safe-lock tube were centrifuged and supernatant was removed. The pellets were flash frozen in liquid nitrogen, and two stainless steel beads (diameter 3.2 mm) were added per tube. The tubes were loaded into a TissueLyser II adapter (pre-cooled in -80 °C) and cracked using a TissueLyser II (QIAGEN) shaking at 30 Hz for 6 minutes. After cracking 1 mL Milli-Q water was added and samples were heated in a 95 °C water bath for 30 minutes. Samples were centrifuged for 30 minutes and the supernatant was filtered (0.2 µm Acrodisc). Samples were stored at -20°C until HPLC analysis.

HPLC analysis was done using two Sugar-Pak I columns (Waters) placed in line in order to get good separation between polyols. A sample volume of 20 µl was injected in the mobile phase consisting of 0.1 mM Ca EDTA in ultrapure water and samples were followed for 30 min. A mixture of trehalose, glucose, glycerol, erythritol, mannitol and arabitol (0.002% – 0.10% w/v) was used as reference. All calibration curves showed an R2 > 0.999 with a limit of detection

Creation of knock-out strains lacking protective proteins

Strains lacking putative protective proteins were made using a CRISPR/Cas9 genome editing protocol described previously [49]. In sort, a target sequence was designed *in silico* using ChopChop predictors [50]. The guide RNA targeting the gene coding for the protective proteins was constructed by PCR and inserted into vector pFC332 using PacI (Fermentas, Thermo Fisher) digestion and subsequent ligation. The newly created plasmids were used for PEG-mediated protoplast transformation, using strain MA234.1 (*ΔkusA*) as the parental strain. Selection was based on hygromycin, and transformants were purified in multiple rounds to lose the CRISPR/Cas9 containing plasmid (see [49] for more details). Genomic DNA was extracted from purified transformants using a phe-

nol-chloroform based protocol [51]. Diagnostic PCR amplifying the deleted region was performed to check for correct deletion of the target gene. All strains created this way are listed in Table 8.3. Primers and plasmids used to create the knock-out strains are listed in Table 8.4 and Table 8.5, respectively.

Table 8.3. Strains used in this study

Strain name	Genotype	Description	Parental strain	Origin
MA234.1	*ΔkusA*	Parental strain for CRISPR/Cas9 genome editing, lacking *kusA* gene.	N402	[69]
SJS143	*ΔNRRL3_01479; 'ΔdprA'*	Strain lacking a gene coding for a putative dehydrin-like protein [62]	MA234.1	This study
SJS144	*ΔNRRL3_01479; 'ΔdprB'*	Strain lacking a gene coding for a putative dehydrin-like protein [62]	MA234.1	This study
SJS145	*ΔNRRL3_01479, ΔNRRL3_01479; 'ΔdprAB'*	Strain lacking both dehydrin-like proteins [62]	MA234.1	This study
SJS146	*ΔNRRL3_05684; 'ΔLEA3-like'*	Strain lacking a LEA3-like protein thought to be involved in the cell stress response [30,63]	MA234.1	This study
SJS147.2	*ΔNRRL3_02511, 'ΔconJ'*	Strain lacking a homologue of *conJ* described in *A. nidulans* involved in stress response [64]	MA234.1	This study
JZ2.1	*ΔNRRL3_11620; 'Δhsp9/12'*	Strain lacking putative Hsp12, important for plasma membrane stability in *S. cerevisiae* [46,65]	MA234.1	This study
JZ3.1	*ΔNRRL3_02725; 'Δhsp104'*	Strain lacking putative Hsp104, important for heat resistance in *S. cerevisiae* [37,48,66]	MA234.1	This study

Table 8.4. Primers used in this study.

Primer name	Sequence	Use
pTE1_for	CCttaattaaACTCCGCCGAACGTACTG	5' gRNA constructs (promotor). Lower-case letters represent PacI cut site.
pTE1_rev	CCttaattaaAAAAGCAAAAAAGGAAGGTACAAAAAAGC	3' gRNA constructs (terminator). Lower-case letters represent PacI cut site.
Con10_fw	AGTGTCGAATATCGCCAAGAGTTTTAGAGCTAGAAATAGC	3' *conJ* gRNA
Con10_rv	TCTTGGCGATATTCGACACTGACGAGCTTACTCGTTTCGT	5' *conJ* gRNA
5_Con10_fw	CCCTGCCATGTAAGTTCCCGCG	5' *conJ* flank (repair DNA fragment)
5_Con10_KORE_rv	GGAGTGGTACCAATATAAGCCGGTGATTCTGATCCAATTCCAAACCTCA	5' *conJ* flank (repair DNA fragment)

Primer name	Sequence	Use
3_Con10_KORE_fw	CCGGCTTATATTGGTACCACTCCTTGAGT-GAAGGTACCGCTGGGA	3' *conJ* flank (repair DNA fragment)
3_Con10_rv	CGTCGAGTTGAAGCGACCGGAA	3' *conJ* flank (repair DNA fragment)
DIAG_Con10_5_fw	TAGCCTAGGCTCCCCTTCCCCA	Diagnostic PCR *conJ* deletion
DIAG_Con10_3_rv	ACGCTGCCGCTTACTGTAGCAC	Diagnostic PCR *conJ* deletion
Lea3_fw	GCCACTGCCCGTCGTGACAAGTTTTA-GAGCTAGAAATAGC	3' *LEA3-like* gRNA
Lea3_rv	TTGTCACGACGGGCAGTGGCGACGAGCT-TACTCGTTTCGT	5' *LEA3-like* gRNA
5_Lea3_fw	GGCAGTTGGACTGGGTTTGGGG	5' *LEA3-like* flank (repair DNA fragment)
5_Lea3_KORE_rv	GGAGTGGTACCAATATAAGCCGGTCAAGTT-GATGGGATTGAGGATGGA	5' *LEA3-like* flank (repair DNA fragment)
3_Lea3_KORE_fw	CCGGCTTATATTGGTACCACTCCGCACGCTT-GACGACCTGCATGA	3' *LEA3-like* flank (repair DNA fragment)
3_Lea3_rv	CCCGGACACTGGCAATTCCGTC	3' *LEA3-like* flank (repair DNA fragment)
DIAG_Lea3_5_fw	TCACCGACCAGGGGAAGGATGC	Diagnostic PCR *LEA3-like* deletion
DIAG_Lea3_3_rv	TGGAGACGATGGGTCCGCATGA	Diagnostic PCR *LEA3-like* deletion
DehydrinA_fw	TGGTCCCCACTCCTCCAACAGTTTTA-GAGCTAGAAATAGC	3' *dprA* gRNA
DehydrinA_rv	TGTTGGAGGAGTGGGGACCAGACGAGCT-TACTCGTTTCGT	5' *dprA* gRNA
5_DehydrinA_fw	ACCCCAGACTTGGACTCGAGGC	5' *dprA* flank (repair DNA fragment)
5_DehydrinA_KORE_rv	GGAGTGGTACCAATATAAGCCGGTGGG-CAATTGTATGTGTGTTTGGT	5' *dprA* flank (repair DNA fragment)
3_DehydrinA_KORE_fw	CCGGCTTATATTGGTACCACTCCGCGGG-CAAACATAAATGCTTGCGT	3' *dprA* flank (repair DNA fragment)
3_DehydrinA_rv	ACGTTCCCGCACACATATGCAT	3' *dprA* flank (repair DNA fragment)
DIAG_DehydrinA_5_fw	GACATCGACGGCACTGGCTGAG	Diagnostic PCR *dprA* deletion
DIAG_DehydrinA_3_rv	CGGAAGGGCTGTTCAACCCACC	Diagnostic PCR *dprA* deletion
DehydrinB_fw	CCAGCGCAACCACTGCAACAGTTTTA-GAGCTAGAAATAGC	3' *dprB* gRNA
DehydrinB_rv	TGTTGCAGTGGTTGCGCTGGGACGAGCT-TACTCGTTTCGT	5' *dprB* gRNA
5_DehydrinB_fw	CCGCAATCCACACTAGGCCGTC	5' *dprB* flank (repair DNA fragment)
5_DehydrinB_KORE_rv	GGAGTGGTACCAATATAAGCCGGAGGTAG-TATCCATTCCCCACCGT	5' *dprB* flank (repair DNA fragment)
3_DehydrinB_KORE_fw	CCGGCTTATATTGGTACCACTCCCGCTATGG-GAATGAACCCCGCC	3' *dprB* flank (repair DNA fragment)

Primer name	Sequence	Use
3_DehydrinB_rv	GAAGATGGAGCACCTCAGGCGC	3' *dprB* flank (repair DNA fragment)
DIAG_DehydrinB_5_fw	GGCGATCGTGGTGCTCTTGAGG	Diagnostic PCR *dprB* deletion
DIAG_DehydrinB_3_rv	AGAGGATTGGGTGCGCTGGAGT	Diagnostic PCR *dprB* deletion
HSF1_fw_1	ACTGGAACTGGAGAAAACGGGTTTTA-GAGCTAGAAATAGCAAG	PCR target 3'flank
HSF1_rv_1	CCGTTTTCTCCAGTTCCAGTGACGAGCT-TACTCGTTTCG	PCR target 5' flank
HSP12_fw_2	CAGCAAGTCCGGTCCCCAGGGTTTTA-GAGCTAGAAATAGCAAG	PCR target 3'flank
HSP12_rv_2	CCTGGGGACCGGACTTGCTGGACGAGCT-TACTCGTTTCG	PCR target 5' flank
HSP104_fw_2	GGATCGAGAAGGGCCGTCGGGTTTTA-GAGCTAGAAATAGCAAG	PCR target 3'flank
HSP104_rv_2	CCGACGGCCCTTCTCGATCCGACGAGCT-TACTCGTTTCG	PCR target 5' flank
NRRL3-02725-5'-fw	ACGTGCTGGTCAAGTGTATCGA	Donor DNA Hsp104 deletion; Diagnostic PCR
NRRL3-02725-5'-rv	GGAGTGGTACCAATATAAGCCGGGGTGGTT-GATGGGTAGATGGAA	Donor DNA Hsp104 deletion
NRRL3-02725-3'-fw	CCGGCTTATATTGGTACCACTCCGGCGGAAT-GTGAGGGAAGAATG	Donor DNA Hsp104 deletion
NRRL3-02725-3'-rv	GCTTGAGCATCCCAAGGAGAGA	Donor DNA Hsp104 deletion; Diagnostic PCR
NRRL3-07278-5'-fw	GAAATCAGGCTTTGGGACAGGC	Donor DNA Hsf1 deletion
NRRL3-07278-5'-rv	GGAGTGGTACCAATATAAGCCGGCGGTCGG-TAAAGAGCAAAGACG	Donor DNA Hsf1 deletion
NRRL3-07278-3'-fw	CCGGCTTATATTGGTACCACTCCTGTGTCCG-CGGAAGGCAATATA	Donor DNA Hsf1 deletion
NRRL3-07278-3'-rv	TAGGCGATGACACAGACCAAGG	Donor DNA Hsf1 deletion
NRRL3-11620-5'-fw	ATGATACTGCGGATGAGGAGGC	Donor DNA Hsp9/12 deletion; Diagnostic PCR
NRRL3-11620-5'-rv	GGAGTGGTACCAATATAAGCCGGCGCCA-CACCCTGATTACAATCG	Donor DNA Hsp9/12 deletion
NRRL3-11620-3'-fw	CCGGCTTATATTGGTACCACTC-CCAAGTTGCTCCATGACGTCGAC	Donor DNA Hsp9/12 deletion
NRRL3-11620-3'-rv	TTTGTCTCCCAAGTAGGCCGAG	Donor DNA Hsp9/12 deletion; Diagnostic PCR

Table 8.5. Plasmids used in this study

Plasmid	Target gene	An# (gene)	Gene name	CRISPR/Cas9 target sequence	Ref.
pTLL108.1	-	-	-	-	[49]
pTLL109.2	-	-	-	-	[49]
pFC332	-	-	-	-	[70]
pFC332_ *con10*-sgRNA	NRRL3_02511	An01g10790	*conJ*	AGTGTCGAATATCGCCAAGA	This study
pFC332_ *lea3*-sgRNA	NRRL3_05684	An02g07350	*LEA3-like*	GCCACTGCCCGTCGTGACAA	This study
pFC332_*dehydrinA*-sgRNA	NRRL3_01017	An14g05070	*dprA*	TGGTCCCCACTCCTCCAACA	This study
pFC332_*dehydrinB*-sgRNA	NRRL3_01479	An13g01110	*dprB*	CCAGCGCAACCACTGCAACA	This study
pHSF1_1	NRRL3_07278	An16g01760	*hsfA*	ACTGGAACTGGAGAAAACGG	This study
pHSP12_2	NRRL3_11620	An06g01610	*hsp9/12*	CAGCAAGTCCGGTCCCCAGG	This study
pHSP104_2	NRRL3_02725	An01g13350	*hsp104*	GGATCGAGAAGGGCCGTCGG	This study

RNA isolation and protein isolation

To obtain dormant conidia, MEA plates were inoculated confluently using sterilized glass beads and incubated at 28°C, 32°C and 37°C for 8 days. Temperatures of the incubators were double-checked with multiple thermometers and settings were adjusted if needed to obtain cultivation temperatures as close as possible to absolute temperatures. Conidia were harvested in cold PS + 0.02% Tween 80 buffer and filtered using sterile filters (Amplitude Ecocloth, CONTEC) into a falcon tube and put directly on ice. In the case of plates cultivated at 37°C, conidia from three plates were pooled (forming 1 pellet) in order to get enough conidia per sample. Samples were centrifuged for 5 minutes at 3000 rpm and 4°C, after which supernatant was removed from the pellets. The pellets were resuspended in 100µL RNAlater (Sigma) and subsequently flash frozen in liquid nitrogen. Stainless steel grinding jars for Tissuelyzer use (QIAGEN) were pre-cooled in a -80°C freezer and kept cold with liquid nitrogen inside a mortar until the flash frozen pellets were added. Cells were broken using a Tissuelyzer II (QIAGEN) shaking for 1 minute at 30 Hz. Crushed samples, while still cold and powdery, were divided between two safe-lock Eppendorf tubes; one meant for proteome analysis (kept in liquid nitrogen

and subsequent -80°C until further analysis) and one for RNA extraction already containing 450 µL RLC buffer from the RNeasy Plant Mini Kit (QIAGEN). RNA extraction and purification was continued following the manual supplied by the manufacturer including the on-column DNA digestion step. RNA quality was assessed on gel and the quantity was determined using Qubit (ThermoFisher). The RNA samples were handed over to the Utrecht Sequencing facility for Illumina NextSeq2000 2x50 paired-end sequencing.

Protein sample preparation

Powdered samples were extracted using an extraction buffer of 1% (w/v) sodium dodecyl sulfate (SDS, Sigma-Aldrich) in 100 mM ammonium bicarbonate (AMBIC, Sigma-Aldrich), by vigorous vortexing and sonication followed by 10 minutes of centrifugation at 10,000 x g to clear the extract. Supernatants were transferred to a fresh tube and their protein content was determined by bicinchoninic acid assay (BCA assay, Thermo Scientific, Etten-Leur, the Netherlands), according to the manufacturer's protocol.

Subsequently, 20 µg of protein for each sample was reduced and alkylated by the addition of 10 mM Tris carboxyethyl phosphine (TCEP, Sigma-Aldrich) and 40 mM chloroacetamide (CAA, Sigma Aldrich) and incubation at 60°C for 30 minutes. Samples were cooled at room temperature and cleaned up using protein aggregation capture on microparticles to remove interfering contaminants such as SDS by protein precipitation [52] on carboxyl modified magnetic beads (1:1 mixture Sera-Mag A and Sera-Mag B Thermo Scientific, Etten-Leur), also called SP3 [53] using improvements described by Sielaff, M *et al.* [54].

In short 20 µg of protein lysate (20 µl) was added to 2 µl (100 µg/µl beads suspension) of carboxyl modified magnetic bead mixture. The mixture was brought to 50% (v/v) acetonitrile (ULC-MS grade, Biosolve) concentration vortex mixed and incubated for 20 minutes at room temperature, after which samples were placed on a magnetic rack. Supernatants were removed and beads were washed twice with 200 µl 70% (v/v) ethanol (HPLC-Grade, Biosolve) on the magnetic rack. Subsequently beads are washed with 180 µl of acetonitrile on the magnetic rack and following removal, air dried. Beads

were resuspended in 20 ul of digestion buffer (100 mM AMBIC), and following addition of 1 µg of trypsin (sequencing grade, Promega, 1:20 enzyme to substrate ratio by weight) and incubation overnight at 37° C. Following digestion, supernatants were acidified by addition of 1% (v/v) formic acid (ULC-MS Biosolve) and careful transfer of peptide containing supernatants to a clean tube after placing samples on a magnetic rack. Cleaned samples were ready for LC-MS analysis.

Mass spectrometry (proteome)

200 ng of peptides were injected onto a 75 µm × 250 mm column (C18, 1.6 µm particle size, Aurora, IonOpticks, Australia) kept at 50 °C at 400 nL/min for 15 min with 3% acetonitrile, 0.1% formic acid in water using an Ultimate 3000 RSLCnano UHPLC system (Thermo Scientific, Germering, Germany). Peptides were subsequently separated by a multi-step gradient to 40% acetonitrile at 90 minutes, 99% acetonitrile at 92 min held until 102 min returning to initial conditions at 105 min and kept there until 120 min to re-equilibrate the column. Eluting peptides were sprayed into a captive spray source (Bruker, Bremen, Germany) with a capillary voltage of 1.5 kV, a source gas flow of 3 L/min of pure nitrogen and a dry temperature setting of 180 °C, attached to a timsTOF pro (Bruker, Bremen, Germany) trapped ion mobility, quadrupole, time of flight mass spectrometer. The timsTOF was operated in PASEF mode of acquisition. The TOF scan range was 100–1700 m/z with a tims range of 0.6–1.6 V·s/cm2. In PASEF mode a filter was applied to the m/z and ion mobility plane to select features most likely representing peptide precursors, the quad isolation width was 2 Th at 700 m/z and 3 Th at 800 m/z, and the collision energy was ramped from 20–59 eV over the tims scan range to generate fragmentation spectra. A total number of 10 PASEF MS/MS scans scheduled with a total cycle time of 1.16 s, scheduling target intensity 2 × 104 and intensity threshold of 2.5 × 103 and a charge state range of 0–5 were used. Active exclusion was on (release after 0.4 min), reconsidering precursors if ratio current/previous intensity >4.

Data analysis (proteome)

Generated mass spectral data were processed using MaxQuant (Version 1.6.10.43),

searching a proteome database of *Aspergillus niger* (Uniprot downloaded September 2019). The proteolytic enzyme was set to trypsin allowing for a maximum of two missed cleavages. Carbamidomethyl (C) was set as a fixed modification Oxidation (M) as a variable modification. Group specific settings was set to timsDDA, and LFQ and iBAQ for quantitation were enabled. Matched between runs was also enabled using the standard settings for matching. Significantly differentially expressed proteins (DEPs) were calculated using the DEP package in R [55] using the user defined cut-offs alpha = 0.05 and lfc = $\log_2(2)$.

Data analysis (transcriptome)

Raw transcriptome data was obtained from the Utrecht Sequencing facility. The fastq files were mapped to the publicly available *A. niger* NRRL3 genome [56] using HISAT2 [57] with setting intron lengths between 20 and 1000 and suppressing SAM records for reads that failed to align. SAM files were turned into BAM files using the view and sort functions of SAMtools [58]. The htseq-count option of the tool HTSEQ [59] was used to create count text files. The count files served as input for the DESeq2 R package [60] using the DEseqDataSetFromHTSeqCount option. Shrunken log fold changes are calculated using the apeglm package [61].

The $\log_2$ fold changes ($\log_2$FC) in transcriptome and proteome data were compared using only 2381 genes (out of the 11863 genes present on the *A. niger* NRRL3 genome) of which both transcriptome and proteome data was available. Enrichment studies were done on the transcriptome dataset. Custom scripts were developed in Python and implemented in a web interface (https://fungalgenomics.science.uu.nl) to analyze over- and under-representation of functional annotation terms in sets of differentially regulated genes using the Fisher Exact test. The Benjamin-Hochberg correction was used to correct for multiple testing using a p-value < 0.05.

References

1. Criado MV, Fernández Pinto VE, Badessari A, Cabral D. Conditions that regulate the growth of moulds inoculated into bottled mineral water. Int J Food Microbiol. 2005;

2. Snyder AB, Churey JJ, Worobo RW. Association of fungal genera from spoiled processed foods with physicochemical food properties and processing conditions. Food Microbiol. 2019;83:211–8.

3. Rico-Munoz E, Samson RA, Houbraken J. Mould spoilage of foods and beverages: Using the right methodology. Food Microbiol. 2019;81:51–62.

4. Pitt JI. Xerophilic fungi and the spoilage of foods of plant origin. In: Duckworth L, editor. Water relations of foods. Elsevier; 1975. p. 273–307.

5. Hess M, Paul SS, Puniya AK, van der Giezen M, Shaw C, Edwards JE, et al. Anaerobic fungi: past, present, and future. Front Microbiol. 2020;11:1–18.

6. Wang M, Jiang X, Wu W, Hao Y, Su Y, Cai L, et al. Psychrophilic fungi from the world's roof. Persoonia Mol Phylogeny Evol Fungi. 2015;34:100–12.

7. Davies CR, Wohlgemuth F, Young T, Violet J, Dickinson M, Sanders JW, et al. Evolving challenges and strategies for fungal control in the food supply chain. Fungal Biol Rev. 2021;36:15–26.

8. Bayne HG, Michener HD. Heat resistance of *Byssochlamys* ascospores. Appl Environ Microbiol. 1979;37:449–53.

9. Rico-Munoz E. Heat resistant molds in foods and beverages: recent advances on assessment and prevention. Curr Opin Food Sci. 2017;17:75–83.

10. Dijksterhuis J. Heat-resistant ascospores. In: Dijksterhuis J, Samson RA, editors. Food Mycol A Multifaceted Approach to Fungi Food. CRC Press; 2007. p. 101–18.

11. Dijksterhuis J. Fungal spores : Highly variable and stress-resistant vehicles for distribution and spoilage. J Food Microbiol. 2019;81:2–11.

12. Wyatt TT, Wösten HAB, Dijksterhuis J. Fungal spores for dispersion in space and time. Adv Appl Microbiol. 2013;85:43–91.

13. Jara D, Portnoy J, Dhar M, Barnes C. Relation of indoor and outdoor airborne fungal spore levels in the Kansas City metropolitan area. Allergy asthma Proc. United States; 2017;38:130–5.

14. Guinea J, Peláez T, Alcalá L, Bouza E. Outdoor environmental levels of *Aspergillus* spp. conidia over a wide geographical area. Med Mycol. 2006;44:349–56.

15. Abu-Dieyeh MH, Barham R, Abu-Elteen K, Al-Rashidi R, Shaheen I. Seasonal variation of fungal spore populations in the atmosphere of Zarqa area, Jordan. Aerobiologia (Bologna).

2010;26:263–76.

16. Kure CF, Skaar I, Brendehaug J. Mould contamination in production of semi-hard cheese. Int J Food Microbiol. 2004;

17. Groot MN, Abee T, van Bokhorst-van de Veen H. Inactivation of conidia from three *Penicillium* spp. isolated from fruit juices by conventional and alternative mild preservation technologies and disinfection treatments. Food Microbiol. 2019;

18. Dijksterhuis J, Meijer M, van Doorn T, Houbraken J, Bruinenberg P. The preservative propionic acid differentially affects survival of conidia and germ tubes of feed spoilage fungi. Int J Food Microbiol. 2019;306:108258.

19. Samson RA, Houbraken J, Thrane U, Frisvad JC, Andersen B. Food and Indoor Fungi. 2nd ed. Samson RA, Houbraken J, Thrane U, Frisvad JC, Andersen B, editors. Utrecht: Centraalbureau voor Schimmelcultures; 2019.

20. Rukke EO, Sørhaug T, Stepaniak L. Heat treatment of milk: Thermization of milk. In: Fuquay JW, Fox PF, McSweeny PLH, editors. Encycl Dairy Sci. 2nd ed. Elsevier Ltd; 2011. p. 693–8.

21. van den Brule T, Punt M, Teertstra W, Houbraken J, Wösten H, Dijksterhuis J. The most heat-resistant conidia observed to date are formed by distinct strains of *Paecilomyces variotii*. Environ Microbiol. 2019;22:986–99.

22. Hallsworth JE, Magan N. Culture Age, temperature, and pH affect the polyol and trehalose contents of fungal propagules. Appl Environ Microbiol. 1996;62:2435–42.

23. Hagiwara D, Sakai K, Suzuki S, Umemura M, Nogawa T, Kato N, et al. Temperature during conidiation affects stress tolerance, pigmentation, and trypacidin accumulation in the conidia of the airborne pathogen *Aspergillus fumigatus*. PLoS One. 2017;12:e0177050.

24. Teertstra WR, Tegelaar M, Dijksterhuis J, Golovina EA, Ohm RA, Wösten HAB. Maturation of conidia on conidiophores of *Aspergillus niger*. Fungal Genet Biol. 2017;98:61–70.

25. Punt M, van den Brule T, Teertstra WR, Dijksterhuis J, den Besten HMW, Ohm RA, et al. Impact of maturation and growth temperature on cell-size distribution, heat-resistance, compatible solute composition and transcription profiles of *Penicillium roqueforti* conidia. Food Res Int. 2020;136:109287.

26. Earl Kang S, Celia BN, Bensasson D, Momany M. Sporulation environment drives phenotypic variation in the pathogen *Aspergillus fumigatus*. G3 Genes|Genomes|Genetics. 2021;11:jkab208.

27. Ruijter GJG, Bax M, Patel H, Flitter SJ, Van De Vondervoort PJI, De Vries RP, et al. Mannitol is required for stress tolerance in *Aspergillus niger* conidiospores. Eukaryot Cell. 2003;2:690–8.

28. Wolschek MF, Kubicek CP. The filamentous fungus *Aspergillus niger* contains two “differentially regulated” trehalose-6-phosphate synthase-encoding genes, *tpsA* and *tpsB*. J Biol Chem. 1997;272:2729–35.

29. Svanström Å, Van Leeuwen MR, Dijksterhuis J, Melin P. Trehalose synthesis in *Aspergillus niger*: Characterization of six homologous genes, all with conserved orthologs in related species. BMC Microbiol. 2014;14:1–16.

30. van Leeuwen MR, Krijgsheld P, Bleichrodt R, Menke H, Stam H, Stark J, et al. Germination of conidia of *Aspergillus niger* is accompanied by major changes in RNA profiles. Stud Mycol. 2013;74:59–70.

31. Suh MJ, Fedorova ND, Cagas SE, Hastings S, Fleischmann RD, Peterson SN, et al. Development stage-specific proteomic profiling uncovers small, lineage specific proteins most abundant in the *Aspergillus fumigatus* conidial proteome. Proteome Sci. 2012;10:30.

32. Hagiwara D, Suzuki S, Kamei K, Gonoi T, Kawamoto S. The role of AtfA and HOG MAPK pathway in stress tolerance in conidia of *Aspergillus fumigatus*. Fungal Genet Biol. 2014;73:138–49.

33. Baltussen TJH, Zoll J, Verweij PE, Melchers WJG. Molecular mechanisms of conidial germination in *Aspergillus* spp. Microbiol Mol Biol Rev. 2019;84:e00049-19.

34. Wang F, Sethiya P, Hu X, Guo S, Chen Y, Li A, et al. Transcription in fungal conidia before dormancy produces phenotypically variable conidia that maximize survival in different environments. Nat Microbiol. 2021;6:1066–81.

35. Bos CJ, Debets AJM, Swart K, Huybers A, Kobus G, Slakhorst SM. Genetic analysis and the construction of master strains for assignment of genes to six linkage groups in *Aspergillus niger*. Curr Genet. 1988;14:437–43.

36. Demirci E, Arentshorst M, Yilmaz B, Swinkels A, Reid ID, Visser J, et al. Genetic characterization of mutations related to conidiophore stalk length development in *Aspergillus niger* laboratory strain N402. Front Genet. 2021;12:581.

37. Sanchez Y, Lindquist S. HSP104 required for induced thermotolerance. Science. 1990;248:1112–5.

38. Singer M, Lindquist S. Thermotolerance in *Saccharomyces cerevisiae*: the Yin and Yang of trehalose. Trends Biotechnol. 1998;16:460–8.

39. Glover J, Lindquist S. Hsp104, Hsp70, and Hsp40: a novel chaperone system that rescues previously aggregated proteins. Cell. 1998;94:73–82.

40. Chowdhary S, Kainth AS, Pincus D, Gross DS. Heat Shock Factor 1 drives intergenic association of its target gene loci upon heat shock. Cell Rep. 2019;26:18.

41. Nicholls S, Leach MD, Priest CL, Brown AJP. Role of the heat shock transcription factor, Hsf1, in a major fungal pathogen that is obligately associated with warm-blooded animals. Mol Microbiol. 2009;74:844.

42. Sorger PK, Pelham HRB. Yeast heat shock factor is an essential DNA-binding protein that exhibits temperature-dependent phosphorylation. Cell. 1988;54:855–64.

43. Solís EJ, Pandey JP, Zheng X, Jin DX, Gupta PB, Airoldi EM, et al. Defining the essential function of yeast Hsf1 reveals a compact transcriptional program for maintaining eukaryotic proteostasis. Mol Cell. 2016;63:60–71.

44. Fabri JHTM, Rocha MC, Fernandes CM, Persinoti GF, Ries LNA, Cunha AF da, et al. The heat shock transcription factor HsfA is essential for thermotolerance and regulates cell wall integrity in *Aspergillus fumigatus*. Front Microbiol. 2021;12:656548.

45. Tapia H, Koshland DE. Trehalose is a versatile and long-lived chaperone for desiccation tolerance. Curr Biol. 2014;24:2758–66.

46. Pacheco A, Pereira C, Almeida M, Sousa M. Small heat-shock protein Hsp12 contributes to yeast tolerance to freezing stress. Microbiology. 2009;155:2021–8.

47. Saleh AA, Gune US, Chaudhary RK, Turakhiya AP, Roy I. Roles of Hsp104 and trehalose in solubilisation of mutant huntingtin in heat shocked *Saccharomyces cerevisiae* cells. Biochim Biophys Acta - Mol Cell Res. 2014;1843:746–57.

48. Elliott B, Haltiwanger RS, Futcher B. Synergy between trehalose and Hsp104 for thermotolerance in *Saccharomyces cerevisiae*. Genetics. 1996;144:923–33.

49. van Leeuwe TM, Arentshorst M, Ernst T, Alazi E, Punt PJ, Ram AFJ. Efficient marker free CRISPR/Cas9 genome editing for functional analysis of gene families in filamentous fungi. Fungal Biol Biotechnol. 2019;6:1–13.

50. Labun K, Montague TG, Krause M, Torres Cleuren YN, Tjeldnes H, Valen E. CHOPCHOP v3: expanding the CRISPR web toolbox beyond genome editing. Nucleic Acids Res. 2019;47:171–4.

51. Arentshorst M, Ram AFJ, Meyer V. Using non-homologous end-joining-deficient strains for functional gene analyses in filamentous fungi. Methods Mol Biol. 2012;835:133–50.

52. Batth TS, Tollenaere MAX, Rüther P, Gonzalez-Franquesa A, Prabhakar BS, Bekker-Jensen S, et al. Protein aggregation capture on microparticles enables multipurpose proteomics sample preparation. Mol Cell Proteomics. 2019;18:1027–35.

53. Hughes CS, Foehr S, Garfield DA, Furlong EE, Steinmetz LM, Krijgsveld J. Ultrasensitive proteome analysis using paramagnetic bead technology. Mol Syst Biol. 2014;10:757.

54. Sielaff M, Kuharev J, Bohn T, Hahlbrock J, Bopp T, Tenzer S, et al. Evaluation of FASP, SP3, and iST protocols for proteomic sample preparation in the low microgram range. J Proteome Res. 2017;16:4060–72.

55. Zhang X, Smits AH, van Tilburg GB, Ovaa H, Huber W, Vermeulen M. Proteome-wide identification of ubiquitin interactions using UbIA-MS. Nat Protoc. 2018;13:530–50.

56. Aguilar-Pontes M V., Brandl J, McDonnell E, Strasser K, Nguyen TTM, Riley R, et al. The gold-standard genome of *Aspergillus niger* NRRL 3 enables a detailed view of the diversity of sugar catabolism in fungi. Stud Mycol. 2018;91:61–78.

57. Kim D, Paggi JM, Park C, Bennett C, Salzberg SL. Graph-based genome alignment and genotyping with HISAT2 and HISAT-genotype. Nat Biotechnol 2019 378. 2019;37:907–15.

58. Li H, Handsaker B, Wysoker A, Fennell T, Ruan J, Homer N, et al. The Sequence Alignment / Map (SAM) format and SAMtools 1000 genome project data processing subgroup. Bioinformatics. 2009;25:2078–9.

59. Anders S, Pyl PT, Huber W. HTSeq—a Python framework to work with high-throughput sequencing data. Bioinformatics. 2015;31:166–9.

60. Love MI, Huber W, Anders S. Moderated estimation of fold change and dispersion for RNA-seq data with DESeq2. Genome Biol 2014 1512. 2014;15:1–21.

61. Zhu A, Ibrahim JG, Love MI. Heavy-tailed prior distributions for sequence count data: removing the noise and preserving large differences. Bioinformatics. 2019;35:2084–92.

62. Hoi JWS, Lamarre C, Beau R, Meneau I, Berepiki A, Barre A, et al. A novel family of dehydrin-like proteins is involved in stress response in the human fungal pathogen *Aspergillus fumigatus*. Mol Biol Cell. 2011;22:1896.

63. Romsdahl J, Blachowicz A, Chiang AJ, Singh N, Stajich JE, Kalkum M, et al. Characterization of *Aspergillus niger* isolated from the international space station. mSystems. 2018;3:e00112-18.

64. Suzuki S, Sarikaya Bayram Ö, Bayram Ö, Braus GH. *conF* and *conJ* contribute to conidia germination and stress response in the filamentous fungus *Aspergillus nidulans*. Fungal Genet Biol. Academic Press; 2013;56:42–53.

65. Sales K, Brandt W, Rumbak E, Lindsey G. The LEA-like protein HSP12 in *Saccharomyces cerevisiae* has a plasma membrane location and protects membranes against desiccation and ethanol-induced stress. Biochim Biophys Acta - Biomembr. 2000;1463:267–78.

66. Sanchez Y, Taulien J, Borkovich KA, Lindquist S. Hsp104 is required for tolerance to many forms of stress. EMBO J. 1992;11:2357.

67. Grigoriev I V., Nikitin R, Haridas S, Kuo A, Ohm R, Otillar R, et al. MycoCosm portal: gearing up for 1000 fungal genomes. Nucleic Acids Res. 2014;42:D699–704.

68. Wong Sak Hoi J, Beau R, Latgé JP. A novel dehydrin-like protein from *Aspergillus fumigatus* regulates freezing tolerance. Fungal Genet Biol. Academic Press; 2012;49:210–6.

69. Park J, Hulsman M, Arentshorst M, Breeman M, Alazi E, Lagendijk EL, et al. Transcriptomic and molecular genetic analysis of the cell wall salvage response of *Aspergillus niger* to the absence of galactofuranose synthesis. Cell Microbiol. 2016;18:1268–84.

70. Nødvig CS, Nielsen JB, Kogle ME, Mortensen UH. A CRISPR-Cas9 system for genetic engineering of filamentous fungi. PLoS One. 2015;10:e0133085.

Additional Files

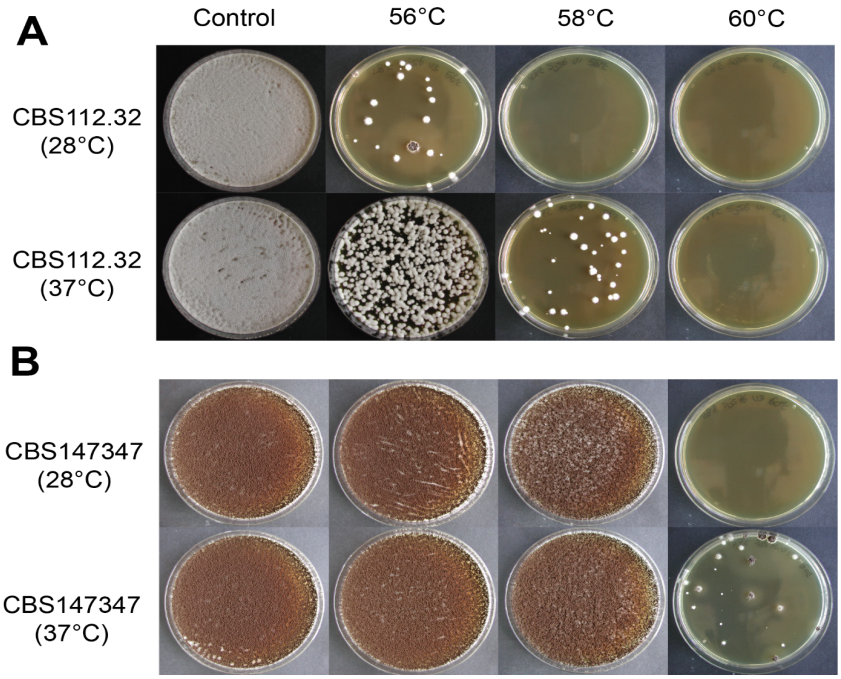

Figure 8.S1. Cultivation temperature impacts heat resistance of wild-type *A. niger* strains CBS112.32 and CBS147347. Heat resistance was investigated using the heat treatment assay, in which conidia are harvested, diluted and subsequently heat treated for 10 minutes in a thermocycler after which 10^6 conidia are plated. Pictures were taken after 5 days of incubation at 28°C. **A.** Heat resistance of wild-type strain *A. niger* CBS112.32. Conidial heat resistance increases when conidia were harvested from plates cultivated at 37°C versus 28°C as seen by the colony forming units obtained after a 10 minutes 58°C heat treatment. **B.** Heat resistance of wild-type strain *A. niger* CBS147347. Conidial heat resistance increases when conidia were harvested from plates cultivated at 37°C versus 28°C as seen by the colony forming units obtained after a 10 minutes 60°C heat treatment.

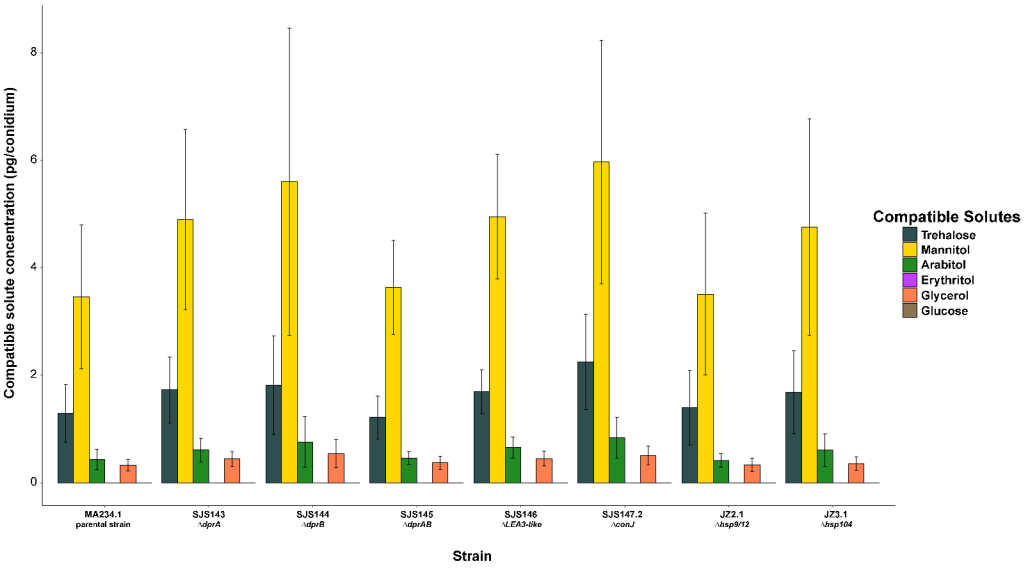

Figure 8.S2. HPLC analysis of knock-out mutants lacking protective proteins. No significant changes in compatible solute compositions were observed in any of the knock-out mutants when compared to the parental strain MA234.1 (*ΔkusA*).

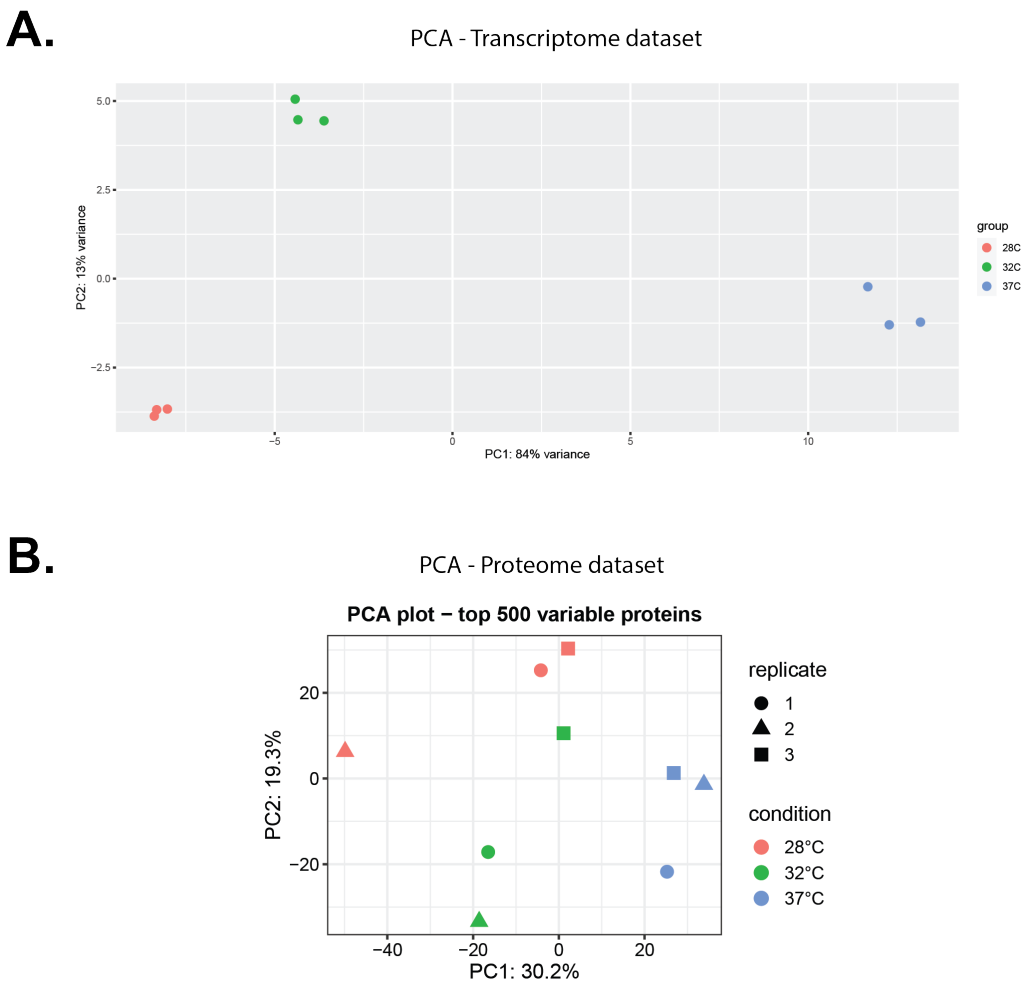

Figure 8.S3. Principle component analysis (PCA) on the transcriptome and proteome datasets. The three cultivation conditions; 28°C, 32°C and 37°C were compared. Most of the variance can be explained by the x-axis, of which the 37°C condition is the largest contributing factor in both cases. **A.** PCA of the transcriptome data, the PCA was made using the DESeq2 package in R [60]. 84% of the variance is found on the x-axis which is mostly due to the 37°C condition. **B.** PCA of the proteome data, the PCA was made using DEP package in R [55]. Variance is not as large as in the transcriptome dataset, but most of it is due to the x-axis difference which is due to the 37°C condition.

Table 8.S1. The 60 proteins significantly more or less present in conidia cultivated at 37°C. Positive values (green) in Log2 fold changes found significant ($p < 0.05$) show upregulation in conidia cultivated at 37°C, whereas negative values (red) show downregulation in conidia cultivated at 37°C. Descriptions are based on EuKaryotic Orthologous Groups (KOG) found as part of MycoCosm on the JGI website [67]. All descriptions are putative and solely based on homology. The baseMean DESeq2 values represent the average of normalized counts and the LFQ intensities represent quantified proteome data based on peptides found (higher values = more protein present). Normalization, Log2FC and their significance were calculated with the DESeq2 package in R for the transcriptome data and the DEP package in R for the proteome data.

			Transcriptome				Proteome		
NRRL3 number	An-number	Description	Base-Mean DESeq2	Log_2FC	p-value	Avg. LFQ intensity 28 °C	Avg. LFQ intensity 37°C	Log_2FC	p-value
NRRL3_10215	An18g00600	Molecular chaperone (small heat-shock protein Hsp26/Hsp42)	12309	2.43	2.44E-44	5900	1178113	7.5	2.6E-13
NRRL3_04002	An15g05410	Molecular chaperone (small heat-shock protein Hsp26/Hsp42)	1759	4.60	1.14E-65	0	130312	7.01	2.2E-08
NRRL3_09378	An11g09460	Sorting nexin SNX11	606	0.17	0.593362	0	97338	5.94	4.9E-04
NRRL3_10516	An18g04270	Parvulin-like peptidyl-prolyl cis-trans isomerase	237	-0.13	0.762198	0	46732	5.85	1.6E-03
NRRL3_11626	An06g01530	Glucan 1,3-beta-glucosidase	33	-0.04	0.940552	2858	196177	5.64	1.3E-06
NRRL3_05700	An02g07130	Mitochondrial large subunit ribosomal protein (Img2)	499	0.94	5.76E-07	0	149847	5.63	3.2E-04
NRRL3_11083	An08g04410	NADH-ubiquinone oxidoreductase subunit	568	-0.50	0.147736	0	125943	5.3	2.7E-03
NRRL3_03693	An15g01410	Possible oxidoreductase	460	0.17	0.626468	0	66393	5.28	1.4E-06
NRRL3_00318	An09g03890	Glyoxylate/ hydroxypyruvate reductase	361	-0.37	0.213897	0	99540	5.27	2.5E-07
NRRL3_11707	An06g00650 An06g00660	Oxoprolinase	1303	0.14	0.652759	218194	349483	5.16	2.0E-07
NRRL3_06627	An16g09040	N-acetyl-glucosamine-6-phosphate deacetylase	1674	-0.13	0.61331	4435	115895	5.05	1.1E-03

			Transcriptome				Proteome		
NRRL3 number	An-number	Description	Base-Mean DESeq2	Log_2FC	p-value	Avg. LFQ intensity 28 °C	Avg. LFQ intensity 37°C	Log_2FC	p-value
NRRL3_08471	An03g04500	Nucleoside diphosphate-sugar hydrolase of the MutT (NUDIX) family	286	-0.24	0.5011	2028	66817	4.85	3.7E-03
NRRL3_07783	An04g05750	hypothetical protein with signal peptide for secretion	460	-0.46	0.089005	0	55409	4.62	1.2E-02
NRRL3_09219	An11g11260	Protein-L-isoaspartate(D-aspartate) O-methyltransferase	3461	0.34	0.188724	11574	171360	4.57	3.6E-02
NRRL3_02034	An01g05040	dUTPase	85	-2.36	0.002346	0	30726	4.56	1.8E-02
NRRL3_07644	An04g07530	G protein-coupled receptor	1954	0.07	0.877749	58759	1304167	4.5	8.7E-03
NRRL3_05517	An02g09030	Nucleolar GTPase/ ATPase p130	27504	-0.22	0.05141	0	58260	4.44	2.1E-02
NRRL3_00602	An14g00300	1-Acyl dihydroxyacetone phosphate reductase and related dehydrogenases	115	-0.08	0.857974	0	40197	4.38	2.7E-02
NRRL3_06470	An17g00880	Damage-control phosphatase ARMT1-like domain	284	0.14	0.575414	0	83084	4.23	8.9E-05
NRRL3_02586	An01g11680	cis-muconate cyclase	170	0.03	0.940182	5144	99614	4.23	3.2E-03
NRRL3_00413	An09g05140	Saccharopine dehydrogenase NADP binding domain	83	-2.28	2.29E-12	0	26898	4.17	7.3E-06
NRRL3_11096	An08g04540	Putative cyclase	83	-0.26	0.561376	4433	80027	4.05	1.5E-02
NRRL3_05056	An02g14900 An02g14910	Ubiquitin activating E1 enzyme-like protein	1866	-0.14	0.415603	#N/A	#N/A	3.56	3.8E-02
NRRL3_04347	An07g01530	GatB domain	63	-0.19	0.666369	26075	258020	3.32	1.1E-02
NRRL3_04490	An07g03340	Fungal hydrophobin *hyp1*	293	0.00	0.995224	539587	5093167	3.26	2.3E-02
NRRL3_09330	An11g09920	Apoptosis-related protein/predicted DNA-binding protein	439	-0.21	0.521993	50923	374457	2.86	4.1E-02

			Transcriptome				Proteome		
NRRL3 number	An-number	Description	Base-Mean DESeq2	Log_2FC	p-value	Avg. LFQ intensity 28 °C	Avg. LFQ intensity 37°C	Log_2FC	p-value
NRRL3_03532	An05g00140	Signal recognition particle receptor, beta subunit (small G protein superfamily)	682	-0.28	0.114883	243067	67113	-2.08	4.2E-02
NRRL3_02666	An01g12550	Mannosyl-oligosaccharide alpha-1,2-mannosidase and related glycosyl hydrolases	3984	-0.66	0.149562	380070	69265	-2.53	5.9E-03
NRRL3_00410	An09g05110	Acyl-CoA synthetase	23559	-1.57	8.83E-05	256357	43786	-2.73	9.1E-03
NRRL3_02657	An01g12450	Chitinase	2316	-2.40	2.9E-05	1256357	176317	-2.83	9.6E-03
NRRL3_06237	An02g00210	Non-ribosomal peptide synthetase/ alpha-aminoadipate reductase and related enzymes	2397	-0.42	0.008291	101361	16332	-2.84	4.2E-02
NRRL3_03373	An12g04700	Dipeptidyl aminopeptidase	154	-0.79	0.069459	231517	34358	-3.04	5.2E-03
NRRL3_10599	An18g05500	Ceramidase	1652	-0.30	0.354418	166843	24713	-3.05	3.3E-02
NRRL3_04237	An07g00110	Beta-lactamase	406	-0.86	0.001611	905467	122393	-3.21	7.8E-03
NRRL3_00071	An09g00810	Zinc-binding oxidoreductase	303	-1.40	2.81E-08	176773	20027	-3.31	2.9E-03
NRRL3_00279	An09g03450	D-ribulose-5-phosphate 3-epimerase	922	-0.57	0.005181	16737	0	-3.49	9.2E-03
NRRL3_06024	An02g02930	ribose-5-phosphate isomerase	2280	-0.30	0.294115	701343	80009	-3.56	1.6E-02
NRRL3_10970	An08g03090	Calcium transporting ATPase	7420	0.15	0.457215	167843	19365	-3.67	4.6E-03
NRRL3_06352	An10g00800	Purine nucleoside permease (NUP)	32	-1.06	0.082256	325673	25999	-3.69	2.0E-04
NRRL3_02923	An12g10470	cyclin-dependent kinase	7273	-0.40	0.166186	1360567	119020	-3.84	3.4E-03
NRRL3_11047	An08g03960	Putative cargo transport protein ERV29	719	-0.39	0.142135	129678	7651	-4.15	2.1E-02
NRRL3_02139	An01g06310	hypothetical protein with DUF1793 domain	98	0.38	0.369748	52896	0	-4.36	3.7E-03
NRRL3_03251	An12g06060	hypothetical protein with YrdC-like domain	301	-1.87	6.26E-11	128167	6207	-4.41	2.2E-06

			Transcriptome				Proteome		
NRRL3 number	An-number	Description	Base-Mean DESeq2	Log_2FC	p-value	Avg. LFQ intensity 28 °C	Avg. LFQ intensity 37°C	Log_2FC	p-value
NRRL3_03449	An12g03850	ATP-dependent RNA helicase	1153	1.15	1.93E-12	42187	0	-4.42	9.7E-04
NRRL3_04236	An07g00100	Amidase	2983	-2.77	2.81E-50	50961	0	-4.5	4.8E-04
NRRL3_10468	An18g03780	Aminopeptidases of the M20 family	672	-0.13	0.662217	337473	14022	-4.58	8.0E-04
NRRL3_06750	An16g07450	Translation initiation factor 2C (eIF-2C) and related proteins	1599	-1.41	1.47E-10	239267	9344	-4.63	3.8E-08
NRRL3_03138	An12g07570	Synaptobrevin/VAMP-like protein	2175	0.97	1.39E-32	120507	2519	-4.73	1.7E-02
NRRL3_06942	An16g04640	Predicted membrane protein	318	0.00	0.998817	53285	0	-4.73	2.3E-02
NRRL3_02536	An01g11100	Predicted membrane protein	8115	0.33	0.011983	40871	0	-4.77	6.9E-03
NRRL3_03346	An12g04950	Mitochondrial F1F0-ATP synthase, subunit epsilon/ ATP15	937	-0.04	0.940168	54565	0	-4.84	2.2E-02
NRRL3_08244	An04g00150	Glutaredoxin-related protein	502	-0.06	0.8883	85849	6223	-4.85	2.4E-02
NRRL3_07734	An04g06310	hypothetical protein with signal peptide for secretion	1476	-0.45	0.000469	61747	0	-5.06	4.3E-02
NRRL3_09480	An11g08250	Glutamate decarboxylase and related proteins	185	-0.90	0.016693	290377	6787	-5.46	1.5E-05
NRRL3_11110	An08g04690	Dehydrogenases with different specificities (related to short-chain alcohol dehydrogenases)	141	-3.62	2.02E-09	192914	3916	-5.59	4.6E-04
NRRL3_04169	An15g07370	Chitinase	26	-0.35	0.414464	111428	0	-5.94	1.5E-06
NRRL3_03454	An12g03760	hypothetical protein	161	2.41	0.000117	1259540	21374	-6.04	2.3E-05
NRRL3_03951	An15g04790	Fungal specific transcription factor domain containing protein	372	0.35	0.135284	165789	0	-6.26	2.6E-03
NRRL3_10314	An18g01890	hypothetical protein	3670	-1.98	2.06E-12	1777000	23598	-6.44	2.6E-13
NRRL3_04228	An07g00020	alpha/beta hydrolase	206	0.35	0.394227	137507	0	-7.7	2.1E-02

Table 8.S2. Transcriptome and proteome changes of all chaperones and potentially protective proteins. Positive values (green) in Log2 fold changes found significant ($p < 0.05$) show upregulation in conidia cultivated at 37°C, whereas negative values (red) show downregulation in conidia cultivated at 37°C. Descriptions are based on EuKaryotic Orthologous Groups (KOG) found as part of MycoCosm on the JGI website [67]. All descriptions are putative and solely based on homology. The baseMean DESeq2 values represent the average of normalized counts and the LFQ intensities represent quantified proteome data based on peptides found (higher values = more protein present). Normalization, Log2FC and their significance were calculated with the DESeq2 package in R for the transcriptome data and the DEP package in R for the proteome data. The #N/A cells represent no proteome data for this gene present.

			Transcriptome				Proteome		
NRRL3 number	**An-number**	**Description**	**Base Mean DESeq2**	**log_2FC (37°C/28°C)**	**p-value**	**Avg.LFQ intensity 28°C**	**Avg. LFQ intensity 37°C**	**log_2FC (37°C/28°C)**	**p-value**
NRRL3_01017	An14g05070	*dprA*. Dehydrin-like protein. Homologue of DprA and DprB from *A. fumigatus*	9697	0.43	0.166	632040	495342	-1.30	0.92
NRRL3_01479	An13g01110	*dprB*. Dehydrin-like protein. Homologue of DprA and DprB from *A. fumigatus* [68]	7317	0.24	0.424	83526	191096	3.29	0.80
NRRL3_05684	An02g07350	LEA3-like protein	10188	0.33	0.2651	2480477	354129	-3.33	0.78
NRRL3_02511	An01g10790	*conJ*. Conidiation factor 10	10603	-2.27	2E-22	14067533	4508780	-2.15	0.859
NRRL3_11620	An06g01610	Heat shock protein 9/12	23695	0.55	0.006	706590	605488	-3.29	0.88
NRRL3_02725	An01g13350	Chaperone Hsp104	17811	-0.04	0.9218	7443467	7087667	-0.18	0.95
NRRL3_07278	An16g01760	Homologue of transcription factor HSF1 from *S. cerevisiae*	2312	0.29	0.0735	17626	26896	0.68	0.94
NRRL3_04002	An15g05410	Small heat-shock protein Hsp26/ Hsp42	1759	4.60	1E-65	0	130312	7.01	0.00
NRRL3_10215	An18g00600	Small heat-shock protein Hsp26/ Hsp42	12309	2.43	2E-44	5900	1178113	7.50	0.00
NRRL3_10695	An18g06650	Small heat-shock protein Hsp26/ Hsp42	374	-0.11	0.7312	#N/A	#N/A	#N/A	#N/A
NRRL3_08747	An03g00400	Small heat-shock protein Hsp26/ Hsp42	353	1.64	8E-10	#N/A	#N/A	#N/A	#N/A
NRRL3_09339	An11g09830	Small heat-shock protein Hsp26/ Hsp42	64	-0.41	0.3087	#N/A	#N/A	#N/A	#N/A
NRRL3_10998	An08g03480	Chaperone Hsp104 /Hsp98	675	-0.65	0.002	468723	441707	-0.19	0.96
NRRL3_10325	An18g02030	Heat shock factor binding protein 1	144	0.33	0.4264	#N/A	#N/A	#N/A	#N/A
NRRL3_00418	An09g05210 An09g05220	Molecular chaperone	1126	0.28	0.267	86884	19907	-2.51	0.27
NRRL3_00872	An14g03220	Molecular chaperone	780	0.41	0.0744	#N/A	#N/A	#N/A	#N/A

			Transcriptome				Proteome		
NRRL3 number	**An-number**	**Description**	**Base Mean DESeq2**	**log_2FC (37°C/28°C)**	**p-value**	**Avg.LFQ intensity 28°C**	**Avg. LFQ intensity 37°C**	**log_2FC (37°C/28°C)**	**p-value**
NRRL3_02772	An01g13900	Molecular chaperone	681	-0.60	0.0779	#N/A	#N/A	#N/A	#N/A
NRRL3_06094	An02g01990	Molecular chaperone	99	-1.19	0.0175	#N/A	#N/A	#N/A	#N/A
NRRL3_07907	An04g04050	Molecular chaperone	63	0.52	0.1181	#N/A	#N/A	#N/A	#N/A
NRRL3_10475	An18g03870	Molecular chaperone	440	-0.78	0.1306	#N/A	#N/A	#N/A	#N/A
NRRL3_10684	An18g06490	Molecular chaperone	648	-0.28	0.4742	11948	36447	0.53	0.96
NRRL3_11344	An08g07800	Molecular chaperone	88	-0.37	0.3794	#N/A	#N/A	#N/A	#N/A
NRRL3_01152	An14g06780	Molecular chaperone	194	0.75	0.0093	#N/A	#N/A	#N/A	#N/A
NRRL3_02701	An01g13070	Molecular chaperone	1111	-0.60	0.0236	145886	101211	-0.59	0.91
NRRL3_08150		Molecular chaperone	285	0.02	0.9815	#N/A	#N/A	#N/A	#N/A
NRRL3_09047	An12g01900	Molecular chaperone	1012	-0.53	0.0008	3182	34725	2.62	0.83
NRRL3_02005	An01g04620	DnaJ domain containing protein	41	-0.29	0.4593	#N/A	#N/A	#N/A	#N/A
NRRL3_00724	An14g01560	Zuotin and related molecular chaperones	730	0.27	0.3174	285847	142623	-0.98	0.82
NRRL3_10682	An18g06470	Zuotin and related molecular chaperones	490	-1.69	4E-13	0	0	#N/A	#N/A
NRRL3_09220	An11g11250	Contains TPR and DnaJ domains	1123	-0.66	9E-06	0	186719	#N/A	#N/A
NRRL3_05015	An07g09990	Molecular chaperones containing Hsp70 protein PFAM domain	53386	-0.12	0.4757	14114333	21501667	0.51	0.92
NRRL3_06609	An16g09260	SSB1 homologue. Molecular chaperones containing Hsp70 protein PFAM domain	10337	0.20	0.4875	15932667	15238667	-0.15	0.96
NRRL3_02714	An01g13220	Molecular chaperones containing Hsp70 protein PFAM domain (GRP170/ SIL1, HSP70 superfamily)	948	-0.49	0.0536	428753	358187	-0.33	0.95
NRRL3_06909	An16g05090	Molecular chaperones containing Hsp70 protein PFAM domain (mortalin/PBP74/ GRP75, HSP70 superfamily)	21561	0.56	1E-07	4467233	6191633	0.41	0.94
NRRL3_09797	An11g04180	Molecular chaperone *bipA*	10667	-1.70	6E-09	525263	1002440	1.06	0.86

			Transcriptome				Proteome		
NRRL3 number	**An-number**	**Description**	**Base Mean DESeq2**	**log_2FC (37°C/28°C)**	**p-value**	**Avg.LFQ intensity 28°C**	**Avg. LFQ intensity 37°C**	**log_2FC (37°C/28°C)**	**p-value**
NRRL3_11153	An08g05300	Molecular chaperones containing Hsp70 protein PFAM domain (HSP105/HSP110/ SSE1, HSP70 superfamily)	6370	-0.01	0.9894	3119067	3696733	0.14	0.96
NRRL3_03649	An15g00900	Metalloprotease with chaperone activity (RNAse H/ HSP70 fold)	223	-0.52	0.0946	#N/A	#N/A	#N/A	#N/A
NRRL3_04460	An07g03020	Metalloprotease with chaperone activity (RNAse H/ HSP70 fold)	285	0.39	0.1662	#N/A	#N/A	#N/A	#N/A
NRRL3_09481	An11g08220	Molecular chaperones containing Hsp70 protein PFAM domain	104	-4.57	5E-17	#N/A	#N/A	#N/A	#N/A
NRRL3_02989		Molecular chaperones containing Hsp70 protein PFAM domain	11	-0.01	0.9894	#N/A	#N/A	#N/A	#N/A
NRRL3_05751	An02g06500	Molecular chaperones containing Hsp70 protein PFAM domain	42	-5.35	0.0004	#N/A	#N/A	#N/A	#N/A
NRRL3_06901	An16g05270	Molecular chaperones containing Hsp70 protein PFAM domain	0	0.00	NA	#N/A	#N/A	#N/A	#N/A
NRRL3_08366	An03g05720	Molecular chaperones containing Hsp70 protein PFAM domain	9	0.48	0.2626	#N/A	#N/A	#N/A	#N/A
NRRL3_09070	An12g01630	Molecular chaperones containing Hsp70 protein PFAM domain	46	-0.01	0.9894	#N/A	#N/A	#N/A	#N/A
NRRL3_10894	An08g02030	Molecular chaperones containing Hsp70 protein PFAM domain	0	0.00	NA	#N/A	#N/A	#N/A	#N/A
NRRL3_10896	An08g02060	Molecular chaperones containing Hsp70 protein PFAM domain	0	0.00	NA	#N/A	#N/A	#N/A	#N/A
NRRL3_02732		Molecular chaperones containing Hsp70 protein PFAM domain	917	0.29	0.1689	#N/A	#N/A	#N/A	#N/A
NRRL3_06378		Molecular chaperones containing Hsp70 protein PFAM domain	9	-0.10	0.7838	#N/A	#N/A	#N/A	#N/A
NRRL3_00540	An09g06590	Molecular chaperone (HSP90 family)	29225	-0.36	0.0091	12163400	15786000	0.35	0.94

			Transcriptome				Proteome		
NRRL3 number	**An-number**	**Description**	**Base Mean DESeq2**	**log_2FC (37°C/28°C)**	**p-value**	**Avg.LFQ intensity 28°C**	**Avg. LFQ intensity 37°C**	**log_2FC (37°C/28°C)**	**p-value**
NRRL3_01036	An14g05320	HSP90 co-chaperone p23	1417	-0.33	0.0691	114657	603870	3.06	0.72
NRRL3_03609	An15g00480	Molecular chaperone (HSP90 family)	949	-0.15	0.6863	#N/A	#N/A	#N/A	#N/A
NRRL3_04680	An07g05920	HSP90 co-chaperone CPR7/ Cyclophilin	1023	0.09	0.7312	334040	554530	0.67	0.86
NRRL3_07788	An04g05700	HSP90 co-chaperone CPR7/ Cyclophilin	84	-0.31	0.3834	#N/A	#N/A	#N/A	#N/A
NRRL3_04490	An07g03340	Fungal hydrophobin *hyp1*/ *hfbC*	293	0.00	0.9952	539587	5093167	3.26	0.02
NRRL3_07571	An04g08500	Fungal hydrophobin *hfbC*-like	100	0.11	0.7865	#N/A	#N/A	#N/A	#N/A
NRRL3_08609	An03g02360	Fungal hydrophobin *hfbB*	1919	-1.25	0.0001	4848300	2510700	-1.10	0.81
NRRL3_08607	An03g02400	Fungal hydrophobin *hfbA*	2443	-1.78	4E-12	1245250	171940	-3.76	0.41
NRRL3_11516	An08g09880	Fungal hydrophobin *hfbD*	9284	-1.01	0.0005	#N/A	#N/A	#N/A	#N/A
NRRL3_03338	An12g05020	Fungal hydrophobin *hfbE*	109	-1.34	0.0179	#N/A	#N/A	#N/A	#N/A
NRRL3_01191	An14g07200	Catalase	11	-0.43	0.3174	#N/A	#N/A	#N/A	#N/A
NRRL3_02898	An12g10720	Catalase	14566	-0.62	7E-12	#N/A	#N/A	#N/A	#N/A
NRRL3_06040	An02g02750	Catalase *catC*	66	0.34	0.4285	0	676	#N/A	#N/A
NRRL3_08371	An03g05660	Catalase	10	-0.28	0.3861	#N/A	#N/A	#N/A	#N/A
NRRL3_11437	An08g08920	Catalase	1939	-1.35	7E-12	1368600	1184940	-0.35	0.94
NRRL3_00252	An09g03130	Catalase *catA*	30191	-0.29	0.0938	6520633	4676600	-0.45	0.94
NRRL3_00644	An14g00690	Catalase	190	-1.38	0.0002	1239393	469803	-1.48	0.51
NRRL3_01760	An01g01550	Catalase *catB*	57	-0.98	0.0775	2619867	2649100	0.04	0.96
NRRL3_01782	An01g01820	Catalase *catR*	37	-0.20	0.6581	6660	22055	0.56	0.95
NRRL3_04527	An07g03770	Super oxide dismutase *sodC*	8566	-0.78	0.0002	1284853	5670500	2.05	0.19
NRRL3_04944	An07g09250	Manganese superoxide dismutase	260	-0.41	0.199	0	9989	#N/A	#N/A
NRRL3_11040	An08g03890	Copper/zinc superoxide dismutase (SODC)	269	-1.23	7E-05	#N/A	#N/A	#N/A	#N/A
NRRL3_02664	An01g12530	Manganese superoxide dismutase	2551	0.25	0.4286	566903	717860	0.22	0.96
NRRL3_07844	An04g04870	Manganese superoxide dismutase	3297	-0.08	0.7549	325160	1082670	1.59	0.61
NRRL3_06880	An16g05520	Copper chaperone for superoxide dismutase	412	-0.88	0.0038	0	0	#N/A	#N/A